

Josephson current in *s*-wave superconductor / Sr_2RuO_4 junctions

Yasuhiro Asano*

Department of Applied Physics, Hokkaido University, Sapporo 060-8628, Japan

Yukio Tanaka

Department of Applied Physics, Nagoya University, Nagoya 464-8603, Japan

Manfred Sigrist

Theoretische Physik ETH-Hönggerberg CH-8093 Zürich, Switzerland

Satoshi Kashiwaya

National Institute of Advanced Industrial Science and Technology, Tsukuba 305-8568, Japan

(Dated: November 11, 2018)

The Josephson current between an *s*-wave and a spin-triplet superconductor Sr_2RuO_4 (SRO) is studied theoretically. In spin-singlet / spin-triplet superconductor junctions, there is no Josephson current proportional to $\sin \varphi$ in the absence of the spin-flip scattering near junction interfaces, where φ is a phase-difference across junctions. Thus a dominant term of the Josephson current is proportional to $\sin 2\varphi$. The spin-orbit scattering at the interfaces gives rise to the Josephson current proportional to $\cos \varphi$, which is a direct consequence of the chiral paring symmetry in SRO.

PACS numbers: 74.80.Fp, 74.25.Fy, 74.50.+r

I. INTRODUCTION

The quantum transport through junctions to unconventional superconductors has attracted much attention in recent years, in particular, in view of various recently discovered compounds belonging probably to this class of systems, such as Sr_2RuO_4 ¹ (SRO), UGe_2 ², ZrZn_2 ³, URhGe ⁴, CeIn_3 and CePd_2Si_2 ⁵. In such systems zero-energy states^{6,7} (ZES) formed at interfaces affect crucially the transport properties through junctions. In normal-metal / high- T_c superconductor⁸ junctions, for instance, a large peak due to the ZES is observed in the conductance at the zero-bias voltage^{9,10,11,12,13,14,15}. The resonant tunneling via the ZES enhances the Andreev reflection¹⁶, which leads to the low-temperature anomaly in the Josephson current, e.g. between two *d*-wave superconductors^{17,18,19,20,21,22,23,24}. The low-temperature anomaly in the Josephson current is a rather common phenomenon for unconventional superconductors including those with spin-triplet pairing²⁵. The possibility of a logarithmic temperature dependence of the critical Josephson current was also predicted for junctions between two SRO samples^{26,27,28}.

The Josephson current-phase relation can be decomposed into a series of contributions of different order

$$J = \sum_{n=1}^{\infty} (J_n \sin n\varphi + I_n \cos n\varphi), \quad (1)$$

where φ is the phase-difference across junctions. The coefficients I_n vanish for all n as long as time reversal symmetry is conserved, since in this case $\varphi \rightarrow -\varphi$ implies $J \rightarrow -J$. As we will deal in the following with a superconducting phase which break time reversal symmetry, we will keep these terms. In the most simple ap-

proach, the lowest order contribution J_1 vanishes, for a junction of the composition spin-singlet superconductor / insulator / spin-triplet superconductor^{29,30,31,32,33,34}, because the wave function of the two superconducting condensates are in orbital and spin part orthogonal to each other. In this case the second order contribution with the Josephson current proportional to $\sin 2\varphi$ is leading. The presence of spin-flip scattering and the breaking of parity at the interface between different materials, would invalidate this simple-minded argumentation. A magnetically active interface yielding spin-flip contributions occurs in the presence of spin-orbit coupling. Obviously, spin-orbit coupling yields new selection rules, because spin and orbital “angular momentum” need not to be conserved independently, but rather only the “total angular momentum” has to remain unchanged in the tunneling process. Then lowest order coupling, J_1 and/or I_1 , can be finite^{25,29,30,34}, so that spin-orbit coupling modifies the current-phase relation of the Josephson effect between singlet and triplet superconductors qualitatively.

In this paper we study the effect of spin-orbit coupling on the Josephson effect for the example of the chiral *p*-wave state which is most likely realized in SRO^{35,36,37,38,39,40,41,42,43,44,45,46,47,48,49,50}. This state breaks time reversal symmetry with an angular momentum along the *c*-axis and has inplane equal spin pairing³⁶. So far the transport properties in junctions consisting of SRO and *s*-wave superconductors or normal metals have been studied in both theories^{51,52,53,54,55,56} and experiments^{57,58,59,60}. The effect of spin-orbit coupling, where it had been taken into account, was introduced in form of effective matrix elements only without the care of a detailed microscopic model for their origin. Here we will consider a model which explicitly introduces spin-orbit coupling as an interface effect and allows us to study

the symmetry related issues of the interface by direct variation of coupling parameters. Our model ignores the spin-orbit coupling effects in the bulk of the two superconductors for the reason that details of the ionic lattice and the band structure would play an essential role, both of which are not easy to implement in a simple model of an unconventional superconductor. Furthermore, we aim here also at effects of the ZES on the Josephson current in connection with the spin-orbit coupling.

This paper is organized as follows. In Sec II, we explain a theoretical model. The Josephson current is derived in Sec. III. The conclusion is given in Sec. IV.

II. ANDREEV REFLECTION COEFFICIENTS

We consider here a junction as shown in Fig. 1 between an *s*-wave superconductor (left hand side) and a *p*-wave superconductor (right hand side) where the later shall be in the chiral *p*-wave state

$$\mathbf{d}(\mathbf{p}) \propto \hat{z}(p_x \pm ip_y) \quad (2)$$

as proposed for SRO. The geometry is chosen so that the current flows in the *x*-direction and the *c*-axis of SRO is in the *z*-direction parallel to the junction interface. Periodic boundary conditions are assumed in the *y*-direction and the width of the junction is *W*, while the system is taken homogeneous along the *z*-direction. The junction is described by the Bogoliubov-de Gennes (BdG) equation⁶¹,

$$\int d\mathbf{r}' \begin{bmatrix} \delta(\mathbf{r} - \mathbf{r}') \hat{h}_0(\mathbf{r}') & \hat{\Delta}(\mathbf{r}, \mathbf{r}') \\ -\hat{\Delta}^*(\mathbf{r}, \mathbf{r}') & -\delta(\mathbf{r} - \mathbf{r}') \hat{h}_0^*(\mathbf{r}') \end{bmatrix} \begin{bmatrix} \hat{u}(\mathbf{r}') \\ \hat{v}(\mathbf{r}') \end{bmatrix} = E \begin{bmatrix} \hat{u}(\mathbf{r}) \\ \hat{v}(\mathbf{r}) \end{bmatrix}, \quad (3)$$

$$\hat{h}_0(\mathbf{r}) = \left[-\frac{\hbar^2 \nabla^2}{2m} - \mu_j + V(\mathbf{r}) \right] \hat{\sigma}_0 + \mathbf{V}(\mathbf{r}) \cdot \hat{\sigma}, \quad (4)$$

$$\hat{\Delta}(\mathbf{R}, \mathbf{r}_r) = \begin{cases} i\mathbf{d}(\mathbf{r}_r) \cdot \hat{\sigma} \hat{\sigma}_2 & \text{for } X_c > L \\ i\mathbf{d}_0(\mathbf{r}_r) \hat{\sigma}_2 & \text{for } X_c < 0 \end{cases}, \quad (5)$$

where $\mathbf{R} = (X_c, Y_c) = (\mathbf{r} + \mathbf{r}')/2$, $\mathbf{r}_r = \mathbf{r} - \mathbf{r}'$. The unit matrix and the Pauli matrices are denoted as $\hat{\sigma}_0$ and $\hat{\sigma}_j$, respectively, with $j = 1, 2$ and 3 . The energy is measured from the chemical potential with $\mu = \mu_S$ for $x < L$ and μ_P for $x > L$, where L is the thickness of the insulator as shown in Fig. 1 (b). The potential of the insulator is given by

$$V(\mathbf{r}) = V_0 [\Theta(x) - \Theta(x - L)], \quad (6)$$

and is in our model also the source of the spin-orbit scattering described by the Hamiltonian

$$H_{so} = -i \left(\frac{\hbar}{2mc} \right)^2 \hat{\sigma} \cdot [\nabla V_0(\mathbf{r}) \times \nabla]. \quad (7)$$

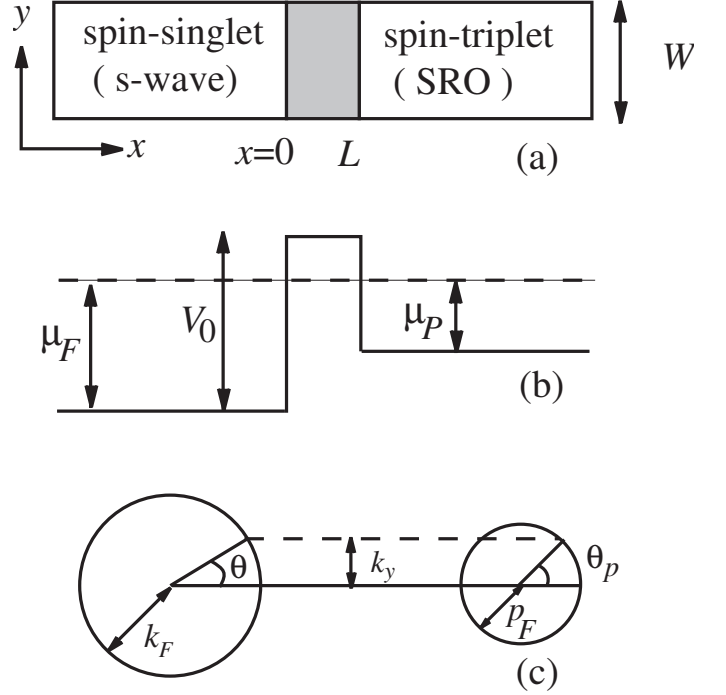


FIG. 1: The *s*-wave superconductor / SRO junction is schematically illustrated in (a). In (b), the broken line indicates the chemical potential of the junction. In (c), we illustrate the Fermi surface in the two superconductors, where θ and θ_p are incident angles of a quasiparticle in *s*-wave superconductor and in SRO, respectively.

Thus the spin-dependent potential in Eq. (4) is described as

$$\mathbf{V}(\mathbf{r}) \cdot \hat{\sigma} = -i \frac{V_0 \alpha_s}{k_F^2} [\delta(x) - \delta(x - L)] \frac{\partial}{\partial y} \hat{\sigma}_3, \quad (8)$$

$$\alpha_s = \left(\frac{\lambda_e k_F}{2} \right)^2, \quad (9)$$

where λ_e is the Compton wavelength and $k_F = \sqrt{2m\mu_S/\hbar^2}$ is the Fermi wave number in the *s*-wave superconductor. The amplitude of the spin-orbit scattering is characterized by the dimensionless coupling constant α_s which is about $10^{-3} \sim 10^{-4}$ in ordinary metals. Throughout this paper, α_s is fixed at 10^{-3} . We assume that all potentials are uniform in superconductors. Therefore the BdG equation can be expressed in the momentum space,

$$\begin{bmatrix} \xi_{\mathbf{k}} \hat{\sigma}_0 & \hat{\Delta}_{\mathbf{k}} \\ -\hat{\Delta}_{-\mathbf{k}}^* & -\xi_{\mathbf{k}} \hat{\sigma}_0 \end{bmatrix} \begin{bmatrix} \hat{u}_{\mathbf{k}} \\ \hat{v}_{\mathbf{k}} \end{bmatrix} = E \begin{bmatrix} \hat{u}_{\mathbf{k}} \\ \hat{v}_{\mathbf{k}} \end{bmatrix}, \quad (10)$$

where we note that $-\hat{\Delta}_{-\mathbf{k}}^* = \hat{\Delta}_{\mathbf{k}}^\dagger$. In the superconductor with unitary pairing states, the amplitudes of the wave

function are given by

$$\begin{bmatrix} \hat{u}_\pm^e \\ \hat{v}_\pm^e \end{bmatrix} = \begin{bmatrix} u_\pm \hat{\sigma}_0 \\ v_\pm \frac{\hat{\Delta}_\pm^\dagger}{|\mathbf{D}_\pm|} \end{bmatrix}, \quad (11)$$

in the electron branch and

$$\begin{bmatrix} \hat{u}_\pm^h \\ \hat{v}_\pm^h \end{bmatrix} = \begin{bmatrix} v_\pm \frac{\hat{\Delta}_\pm}{|\mathbf{D}_\pm|} \\ u_\pm \hat{\sigma}_0 \end{bmatrix}, \quad (12)$$

in the hole branch. In the *s*-wave superconductor, the pair potential and the amplitudes of the wave function in Eqs. (11) and (12) are defined by

$$\hat{\Delta}_\pm = i\Delta_s \hat{\sigma}_2 e^{i\varphi_s}, \quad (13)$$

$$u_\pm = u_s = \sqrt{\frac{1}{2} \left(1 + \frac{\Omega_s}{\omega_n} \right)}, \quad (14)$$

$$v_\pm = v_s = \sqrt{\frac{1}{2} \left(1 - \frac{\Omega_s}{\omega_n} \right)}, \quad (15)$$

$$\Omega_s = \sqrt{\omega_n^2 + \Delta_s^2}, \quad (16)$$

$$|\mathbf{D}_\pm| = \Delta_s, \quad (17)$$

where φ_s is a phase of the pair potential in the *s*-wave superconductor, $\omega_n = (2n+1)\pi k_B T$ is the fermionic Matsubara frequency, k_B is the Boltzmann constant and T is a temperature. For the chiral *p*-wave superconductor, we define now

$$\mathbf{d}(\mathbf{k}) = \Delta_p (\tilde{p}_x + i\tilde{p}_y) e^{i\varphi_p} \mathbf{z} \quad : (p_x + ip_y - \text{symmetry}), \quad (18)$$

where φ_p is the order parameter phase, $\tilde{p}_x = p_x/p_F$, $\tilde{p}_y = p_y/p_F$ and $p_F = \sqrt{2m\mu_P/\hbar^2}$ is the Fermi wavenumber on the right hand side. The amplitudes of the wave function in Eqs. (11) and (12) are given by

$$u_\pm = u_p = \sqrt{\frac{1}{2} \left(1 + \frac{\Omega_p}{\omega_n} \right)}, \quad (19)$$

$$v_\pm = u_p = \sqrt{\frac{1}{2} \left(1 - \frac{\Omega_p}{\omega_n} \right)}, \quad (20)$$

$$\Omega_p = \sqrt{\omega_n^2 + \Delta_p^2}, \quad (21)$$

$$\hat{\Delta}_\pm = i\mathbf{d}_\pm \cdot \hat{\sigma} \hat{\sigma}_2, \quad (22)$$

$$\mathbf{d}_\pm = \Delta_p (\pm \tilde{p}_x + i\tilde{p}_y) e^{i\varphi_p} \mathbf{z}, \quad (23)$$

$$|\mathbf{D}_\pm| = \Delta_p. \quad (24)$$

A condition for the formation of the ZES at the surface of unconventional superconductors is given by²⁵

$$\mathbf{d}_- \mathbf{d}_+ < 0. \quad (25)$$

In the *p*-wave superconductor, Eq. (25) is satisfied only when a quasiparticle is incident perpendicular to the junction interface, (i.e., $\tilde{p}_y = 0$). For other momentum

directions subgap states at finite energy appear forming a gapless chiral quasiparticle spectrum. The wave function in the *s*-wave superconductor $\Psi^s(\mathbf{r})$ and in the *p*-wave superconductor $\Psi^p(\mathbf{r})$ can be represented by Eqs. (13)-(24). In the presence of the spin-orbit scattering, as shown in Eq. (8), the wave functions in the two superconductors are connected with the wave function in the insulator $\Psi^b(\mathbf{r})$ via the boundary conditions,

$$\Psi^b(0, y) = \Psi^s(0, y), \quad (26)$$

$$\begin{aligned} \frac{d}{dx} \Psi^b(x, y) \Big|_{x=0} &= \frac{d}{dx} \Psi^s(x, y) \Big|_{x=0} \\ &+ \bar{V}_0 \alpha_s k_y \check{S}_3 \Psi^s(0, y), \end{aligned} \quad (27)$$

$$\Psi^b(L, y) = \Psi^s(L, y), \quad (28)$$

$$\begin{aligned} \frac{d}{dx} \Psi^b(x, y) \Big|_{x=L} &= \frac{d}{dx} \Psi^p(x, y) \Big|_{x=L} \\ &+ \bar{V}_0 \alpha_s k_y \check{S}_3 \Psi^p(L, y), \end{aligned} \quad (29)$$

$$\check{S}_3 = \begin{pmatrix} \hat{\sigma}_3 & 0 \\ 0 & -\hat{\sigma}_3 \end{pmatrix}. \quad (30)$$

Since α_s is a small value, we calculate the Andreev reflection coefficients within the first order of α_s . From Eqs. (26)-(29), the Andreev reflection coefficients of a quasiparticle incident from a *s*-wave superconductor are calculated as

$$\hat{r}^{he} = \begin{pmatrix} 0 & r^{he}(\uparrow, \downarrow) \\ r^{he}(\downarrow, \uparrow) & 0 \end{pmatrix}, \quad (31)$$

$$\hat{r}^{eh} = \begin{pmatrix} 0 & r^{eh}(\uparrow, \downarrow) \\ r^{eh}(\downarrow, \uparrow) & 0 \end{pmatrix}, \quad (32)$$

$$r^{he}(\downarrow, \uparrow) = \frac{X}{\Xi_+} [-u_s v_s + u_p \tilde{v}_p f_1], \quad (33)$$

$$r^{eh}(\uparrow, \downarrow) = \frac{X}{\Xi_+} [-u_s v_s - u_p \tilde{v}_p f_1^*], \quad (34)$$

$$r^{he}(\uparrow, \downarrow) = \frac{X}{\Xi_-} [u_s v_s + u_p \tilde{v}_p f_1], \quad (35)$$

$$r^{eh}(\downarrow, \uparrow) = \frac{X}{\Xi_-} [u_s v_s - u_p \tilde{v}_p f_1^*], \quad (36)$$

with

$$\tilde{v}_p = v_p e^{-i\theta_p}, \quad (37)$$

$$f_1 = u_s^2 e^{i\varphi} - v_s^2 e^{-i\varphi}, \quad (38)$$

$$X = 4k_F q^2, \quad (39)$$

$$\begin{aligned} \Xi_\pm &= Z_\pm (u_p^2 + \tilde{v}_p^2) (u_s^2 - v_s^2) \\ &+ X [u_p^2 u_s^2 - \tilde{v}_p^2 v_s^2 - 2i u_p \tilde{v}_p u_s v_s \sin \varphi], \end{aligned} \quad (40)$$

$$Z_\pm = z_0 + X \mp \bar{V}_0 \alpha_s q \sin \theta \sinh(2qk_F L) \delta\mu, \quad (41)$$

$$z_0 = \bar{V}_0 (\bar{V}_0 - \delta\mu) \sinh^2(qk_F L) + (k - p)^2 q^2 \quad (42)$$

where $\varphi = \varphi_s - \varphi_p$, $\bar{V}_0 = V_0/\mu_S$ and $\delta\mu = (\mu_S - \mu_P)/\mu_S$. In what follows, we measure the energy in units of μ_S and the length in units of $1/k_F$. The wave numbers in

the x direction are normalized as

$$k = k_x/k_F = \cos \theta \quad (\text{s-wave}), \quad (43)$$

$$q = q_x/k_F = \sqrt{\bar{V}_0 - \cos^2 \theta} \quad (\text{insulator}), \quad (44)$$

$$p = p_x/k_F = \sqrt{\cos^2 \theta - \delta\mu} \quad (\text{SRO}). \quad (45)$$

The incident angle of a quasiparticle in the s -wave superconductor is θ and in the p -wave superconductor $\theta_p = \arctan(k_y/p_x)$ as depicted in Fig. 1 (c).

III. JOSEPHSON CURRENT

The Josephson current is expressed in terms of the Andreev reflection coefficients^{25,62}

$$J = \frac{e}{2\hbar} T \sum_{\omega_n} \mathbf{I}, \quad (46)$$

$$\mathbf{I} = \frac{N_c}{2} \int_{-\theta_0}^{\theta_0} d\theta \cos \theta \frac{1}{\Omega_s} \text{Tr} \left[\hat{\Delta}_s \hat{r}^{he} - \hat{\Delta}_s^\dagger \hat{r}^{eh} \right], \quad (47)$$

where $\theta_0 = \arccos(\delta\mu)$ and $N_c = Wk_F/\pi$ is the number of propagating channels on the Fermi surface. In what follows, we take the units of $\hbar = k_B = 1$. The transmission probability of the junction (g_J) is given by

$$g_J = \int_0^{\theta_0} d\theta \cos \theta T_N, \quad (48)$$

$$T_N = \frac{X}{z_0 + X}, \quad (49)$$

and $G_J = R_J^{-1} = (2e^2/h)N_c g_J$ is the normal conductance of the junction.

We first consider the Josephson effect in the absence of the potential barrier, (i.e., $z_0 = 0$). In Fig. 2 (a), we show the Josephson current as a function of φ , where $\delta\mu = 0$, $k_F L = 0$ and the integration with respect to θ in Eq. (47) is carried out numerically. For simplicity we assume $\Delta_s = \Delta_p$ and describe the temperature dependence of the pair potential by using the BCS theory. The pair potential at $T = 0$ is denoted by Δ_0 . In this case, $g_J = 1$ and there is no spin-orbit scattering at the junctions. The Josephson current is proportional to $\sin 2\varphi$ for high temperatures such as $T/T_c = 0.2 \sim 0.8$ in (a). In a very low temperature, $T/T_c = 0.01$ proportional to $\sin 4\varphi$ slightly modifies the phase-current relationship. The maximum amplitude of the Josephson current increases monotonically with decreasing temperatures as shown in Fig. 2 (b).

Since electronic structures in s -wave superconductor are different from those in SRO, complete transparency of the interface is unrealistic for real junctions. Moreover, we consider an insulating layer between the two superconductors. The calculated results are shown in Fig. 3, where $\bar{V}_0 = 5.0$, $k_F L = 0.6$. We introduce a finite difference of the chemical potentials on both sides of the junction, $\delta\mu = 0.5$. This is necessary to break the

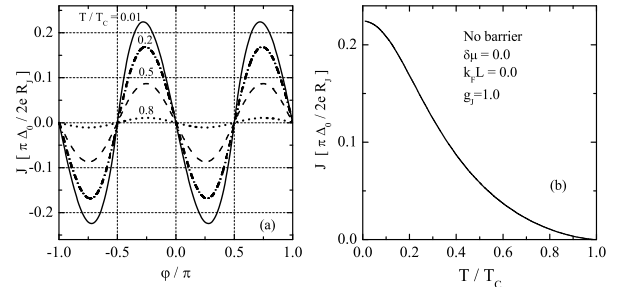


FIG. 2: The Josephson current in s -wave superconductor / SRO is plotted as a function of a phase-difference across junctions for several choices of temperatures in (a), where $z_0 = 0.0$ and $\Delta_s = \Delta_p$. In (b), the maximum Josephson current is plotted as a function of temperatures.

symmetry of the junction, otherwise the orbital parts of different parity would still be orthogonal. With these parameters, the transmission probability is calculated to be $g_J \approx 0.1$. The phase-current relationship is almost described by $J \propto \sin 2\varphi$ even in the presence of the spin-orbit scattering. Since α_s is the small constant, effects of the spin-orbit scattering are still negligible in Fig. 3.

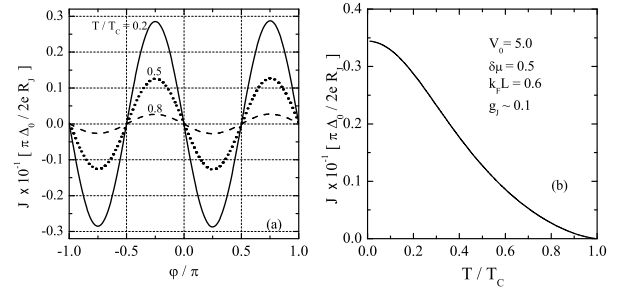


FIG. 3: The Josephson current in s -wave superconductor / SRO is plotted as a function of φ for several choices of temperatures in (a), where $\bar{V}_0 = 5.0$, $\delta\mu = 0.5$ and $k_F L = 0.6$. In (b), the maximum Josephson current is plotted as a function of temperatures.

Next we consider the Josephson effect in the limit of $g_J \ll 1$. The results in such junctions are shown in Fig. 4, where $\bar{V}_0 = 5.0$ and $\delta\mu = 0.5$. The thickness of the insulator $k_F L = 1.72$ is much larger than that in Fig. 3 and g_J is about 0.001. In Fig. 4 (a), the phase current relationship deviates substantially from $\sin 2\varphi$ because of the spin-orbit scattering. At the zero temperature, the

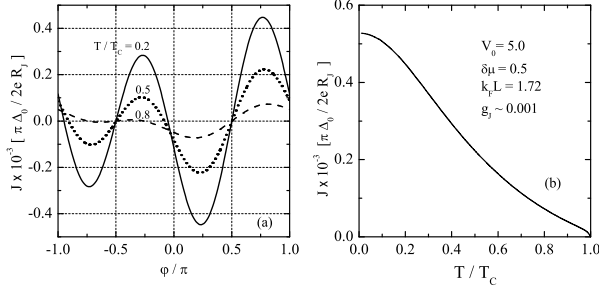


FIG. 4: The Josephson current in s -wave superconductor / SRO is plotted as a function of φ for several choices of temperatures in (a), where $\bar{V}_0 = 5.0$, $\delta\mu = 0.5$ and $k_F L = 1.72$. In (b), the maximum Josephson current is plotted as a function of temperatures.

Josephson current can be roughly expressed by

$$J \sim - \int_0^{\theta_0} d\theta \cos \theta [\delta\mu\alpha_s T_N \cos \varphi + T_N^2 \sin 2\varphi], \quad (50)$$

where $T_N \sim X/z_0$ because of $z_0 \sim \bar{V}_0^2 \exp(2\sqrt{\bar{V}_0} L k_F) \gg X$. The first term is coming from the spin-orbit scattering and is proportional to $\cos \varphi$. In Eq.(1), J_1 and I_1 are proportional to T_N , therefore they are proportional to g_J because a quasiparticle travels twice across the junction to contribute to J_1 or I_1 . A quasiparticle goes across the barrier four times to contribute to the Josephson current proportional to $\sin 2\varphi$. Thus the second term of Eq. (50) is proportional to T_N^2 . Generally speaking, J_n and I_n are proportional to T_N^n and g_J^n . In order to observe the first term in experiments, the transmission probability of the junction must be small enough to satisfy a relation

$$\delta\mu\alpha_s \exp(2\sqrt{\bar{V}_0} L k_F) \sim 1. \quad (51)$$

The left hand side of Eq. (51) is 0.007 in Fig. 3 and 1.1 in Fig. 4. To compare with experiments, Eq. (51) should be put in another way,

$$\frac{J_c}{(\pi\Delta_0/2eR_J)} \leq \alpha_s \sim 10^{-3}, \quad (52)$$

where J_c is the critical Josephson current. In addition to this, the first term becomes more dominant at temperatures close to T_c as shown in Fig. (4) (a). In this junction, there are ZES states. However, there is no anomalous behavior of the Josephson current even in low temperatures as shown in Fig. (4) (b). As we see shortly this aspect can be attributed to the fact, that it is the p_y (the transverse component of the pair wave function) which yields the coupling to the s -wave superconductor through spin-orbit scattering. According to Eq.(25), however, only the p_x -component generates the ZES, which couples in higher

order only. A similar behavior can be found in Josephson effects in SRO/I/SRO junctions, where the two superconductors are belonging to the different chirality^{26,27}.

The energy of the junction can be calculated from the current-phase relationship by using a relation $J = e\partial_\varphi E(\varphi)$. In Fig. 5, we schematically illustrate the energy as a function of φ . When the contribution of the spin-orbit scattering is negligible, there are two energy minima at $\varphi = \pm\pi/2$ as shown with the solid line. These bistable states may be used as a base of the quantum computing devices⁶³. The spin-orbit scattering breaks the bistability as shown with the broken line, where energy at $\varphi = \pi/2$ is slightly smaller than that at $\varphi = -\pi/2$. The energy minima do not shift away from $\varphi = \pm\pi/2$ even in the presence of the spin-orbit scattering. Thus, in the absence of the Josephson current, the phase-difference of junction is considered to be either $\pi/2$ or $-\pi/2$. In experiments, the effects of the spin-orbit scattering may be measured from the difference in the critical Josephson current starting from two different energy minima. An alternative method to confirm the effects of the spin-orbit scattering is the measurement of the Shapiro step in I-V curve. It is also possible to observe directly the phase-current relationship²³.

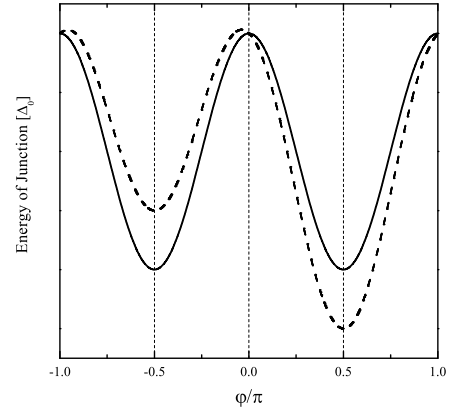


FIG. 5: The energy of the junctions is estimated by using the phase-current relationship. We omit the contribution of the spin-orbit scattering in the solid line. The spin-orbit scattering is taken into account in the broken line.

To understand more clearly the relation between the $p_x + ip_y$ symmetry and the phase-current relationship, we have also calculated the Josephson current in s -wave superconductor/ p -wave superconductor junctions with other pairing symmetries such as

$$\mathbf{d}_\pm = \pm \Delta_p \tilde{p}_x e^{i\varphi_p} \mathbf{z} \quad : (p_x - \text{symmetry}), \quad (53)$$

and

$$\mathbf{d}_\pm = \Delta_p \tilde{p}_y e^{i\varphi_p} \mathbf{z} \quad : (p_y - \text{symmetry}). \quad (54)$$

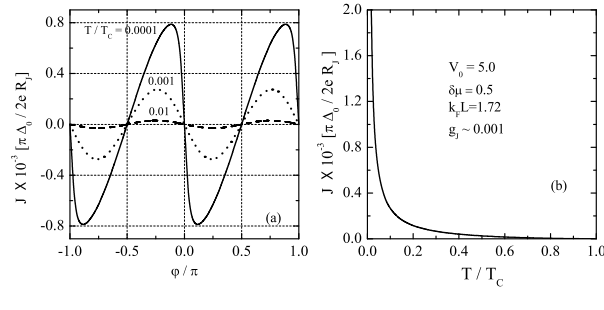


FIG. 6: The Josephson current in s -wave superconductor / p_x -wave superconductor junctions is plotted as a function of φ for several choices of temperatures in (a), where $\bar{V}_0 = 5.0$, $\delta\mu = 0.5$ and $k_F L = 1.72$. In (b), the maximum Josephson current is plotted as a function of temperatures.

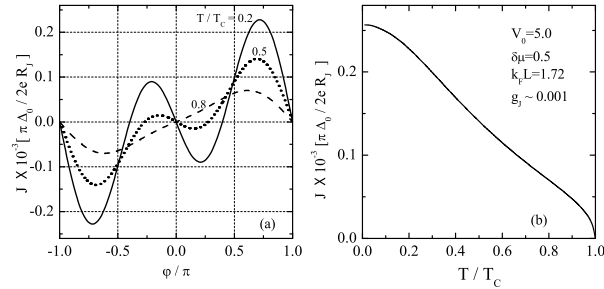


FIG. 7: The Josephson current in s -wave superconductor / p_y -wave superconductor junctions is plotted as a function of φ for several choices of temperatures in (a), where $\bar{V}_0 = 5.0$, $\delta\mu = 0.5$ and $k_F L = 1.72$. In (b), the maximum Josephson current is plotted as a function of temperatures.

In the case of p_x -wave symmetry, the Josephson current in low transparent junctions is shown Fig. 6, where $\bar{V}_0 = 5.0$, $\delta\mu = 0.5$ and $k_F L = 1.72$. The analytical expression at $T = 0$ is given by

$$J \sim -\frac{1}{z_0} \operatorname{sgn}(\varphi) \cos \varphi. \quad (55)$$

In this case, the spin-orbit scattering gives neither J_1 nor I_1 . At very low temperatures, the Josephson current deviates from $\sin 2\varphi$ because higher harmonics J_{2n} with $n \geq 2$ in Eq. (1) contributes to the Josephson current as shown in Fig. 6 (a). Because the condition in Eq. (25)

is fulfilled for all incident angles of a quasiparticle, the ZES are formed at the interface. As a consequence, the Josephson current shows the low-temperature anomaly and increases in proportional to $1/T$ with decreasing temperatures as shown in Fig. 6 (b)^{17,18,22}.

In p_y -wave symmetry, the Josephson current is plotted as a function of φ in Fig. 7 (a), where $\bar{V}_0 = 5.0$, $\delta\mu = 0.5$ and $k_F L = 1.72$. The corresponding analytical result at $T = 0$ is given by

$$J \sim - \int_0^{\theta_0} d\theta \cos \theta [-\delta\mu \alpha_s T_N \sin \varphi + T_N^2 \sin 2\varphi]. \quad (56)$$

In this case, the spin-orbit scattering gives rise to the Josephson current proportional to $\sin \varphi$ which becomes dominant in high temperatures as shown in Fig. 7 (a). Because the condition in Eq. (25) is not satisfied, there is no low-temperature anomaly in the Josephson current as shown in Fig. 7 (b).

IV. CONCLUSION

Finally we summarize the results in this paper. We calculated the Josephson current in s -wave superconductor / SRO by assuming the pair potential in Eq. (23) and compare the results with another pairing symmetries as shown in Eqs. (53) and (54). When the triplet superconductors are described by p_x -wave symmetry, we find the low-temperature anomaly in the Josephson current because the ZES are formed at the interface. We also find in p_x -wave symmetry that effects of the spin-orbit scattering on the Josephson current are absent. It is obvious that spin-orbit coupling is associated with the transverse component p_y , which does not induce a ZES at the interface and consequently does not display the anomalous low-temperature behavior of the maximal Josephson current. Thus, the current-phase relation of the junction is connected with the order parameter phase of the transverse component. This in the case of Eq. (54) φ_p and $\varphi_p + \pi/2$ for Eq. (23), since for the latter the p_y -component is multiplied by i in our definition. This finding of the coupling is entirely in agreement with the qualitative statements of previous discussions of the Josephson effect of this kind, mediated via spin-orbit coupling^{29,30,31,32,33,34}. Furthermore, from Eqs.(50,56) we can conclude, that beyond the finite spin-orbit coupling represented by the coupling constant α_s also the broken parity at the interface, i.e. $\delta\mu \neq 0$ is essential for a finite contribution through this channel.

* Electronic address: asano@eng.hokudai.ac.jp

¹ Y. Maeno, H. Hashimoto, K. Yoshida, S. Nishizaki, T. Fujita, J. G. Bednorz, and F. Lichtenberg, *Nature* **372**, 532

(1994).

² S. S. Saxena, P. Agarwal, K. Ahilan, F. M. Grosche, R. K. W. Haselwimmer, M. J. Steiner, E. Pugh,

I. R. Walker, S. R. Julian, P. Monthoux, G. G. Lonzarich, A. Huxley, I. Sheikin, D. Braithwaite and J. Flouquet, *Nature* **406**, 587 (2000).

³ C. Pfleiderer, M. Uhlarz, S. M. Hayden, R. Vollmer, H. v. Lohneysen, N. R. Bernhoeft, G. G. Lonzarich, *Nature* **412**, 58 (2001).

⁴ D. Aoki, A. Huxley, E. Ressouche, D. Braithwaite, J. Flouquet, J.-P. Brison, E. Lhotel and C. Paulsen, *Nature* **413**, 613 (2001).

⁵ N.D. Mathur et al., *Nature* **394**, 39 (1998).

⁶ C. R. Hu, *Phys. Rev. Lett.* **72**, 1526 (1994).

⁷ L. J. Buchholtz and G. Zwicknagl, *Phys. Rev. B* **23** 5788 (1981).

⁸ J. G. Bednorz and K. A. Müller, *Z. Phys. B* **64**, 189 (1986).

⁹ Y. Tanaka and S. Kashiwaya, *Phys. Rev. Lett.* **74**, 3451 (1995).

¹⁰ S. Kashiwaya and Y. Tanaka, *Rep. Prog. Phys.* **63**, 1641 (2001).

¹¹ S. Kashiwaya, Y. Tanaka, M. Koyanagi and K. Kajimura, *Phys. Rev. B* **53**, 2667 (1996).

¹² S. Kashiwaya, Y. Tanaka, M. Koyanagi, H. Takashima and K. Kajimura, *Phys. Rev. B* **51**, 1350 (1995).

¹³ Y. Tanuma, Y. Tanaka, M. Yamashiro, and S. Kashiwaya, *Phys. Rev. B* **57**, 7997 (1998).

¹⁴ J. Y. T. Wei, N. -C. Yeh, D. F. Garrigus, and M. Strasik, *Phys. Rev. Lett.* **81**, 2542 (1998).

¹⁵ I. Iguchi, W. Wang, M. Yamazaki, Y. Tanaka, and S. Kashiwaya, *Phys. Rev. B* **62**, R6131 (2000).

¹⁶ A. F. Andreev, *Zh. Eksp. Theor. Fiz.* **46**, 1823 (1964) [Sov. Phys. JETP **19**, 1228 (1964)].

¹⁷ Y. Tanaka and S. Kashiwaya, *Phys. Rev. B* **53**, R11957 (1996).

¹⁸ Y. Tanaka and S. Kashiwaya, *Phys. Rev. B* **56**, 892 (1997).

¹⁹ Y. Tanaka and S. Kashiwaya, *Phys. Rev. B* **58**, 2948 (1998).

²⁰ Y. Tanaka and S. Kashiwaya, *J. Phys. Soc. Jpn.* **68**, 3485 (1999).

²¹ Y. Tanaka and S. Kashiwaya, *J. Phys. Soc. Jpn.* **69**, 1152 (2000).

²² Y. S. Barash, H. Burkhardt, and D. Rainer, *Phys. Rev. Lett.* **77**, 4070 (1996).

²³ E. Il'ichev, V. Zakosarenko, R. P. J. IJsselsteijn, V. Schultze, H. -G. Meyer, H. E. Hoenig, H. Hilgenkamp, and J. Mannhart, *Phys. Rev. Lett.* **81**, 894 (1998); E. Il'ichev, M. Grajcar, R. Hlubina, R. P. J. IJsselsteijn, H. E. Hoenig, H. -G. Meyer, A. Golubov, M. H. S. Amin, A. M. Zagoskin, A. N. Omelyanchouk, and M. Yu. Kupriyanov, *Phys. Rev. Lett.* **86**, 5369 (2001).

²⁴ Y. Asano, *Phys. Rev. B* **64**, 014511 (2001); **63**, 052512 (2001).

²⁵ Y. Asano, *Phys. Rev. B* **64**, 224515 (2001).

²⁶ Y. S. Barash, A. M. Bobkov and M. Fogelström, *Phys. Rev. B* **64**, 214503 (2001).

²⁷ Y. Asano and K. Katabuchi, *J. Phys. Soc. Jpn.* **71**, 1974 (2002).

²⁸ R. Mahmoodi, S. N. Shevchenko and Yu. A. Kolesnichenko, *Sov. J. Low Temp. Phys.* **28**, 262 (2002).

²⁹ V.B. Geshkenbein and A.I. Larkin, *Pis'ma Zh. Eksp. Teor. Fiz.* **43**, 306 (1986) [JETP Lett. **43**, 395 (1986)].

³⁰ A. Millis, D. Rainer, and J. A. Sauls, *Phys. Rev. B* **38**, 4504 (1988).

³¹ S. Yip, *J. Low Temp. Phys.* **91**, 203 (1993).

³² J. A. Pals, W. van Haeringen, and M. H. van Maaren, *Phys. Rev. B* **15**, 2592 (1977).

³³ E.W. Fenton, *Solid State Commun.* **54**, 709 (1985); **60**, 347 (1986).

³⁴ M. Sigrist and K. Ueda, *Rev. Mod. Phys.* **63**, 239 (1991).

³⁵ F. Laube, G. Goll, H. v. Löhneysen, M. Fogelström and F. Lichtenberg, *Phys. Rev. Lett.* **84**, 1595 (2000).

³⁶ T. M. Rice and M. Sigrist, *J. Phys. Condens. Matter* **7**, L643 (1995).

³⁷ I. I. Mazin and D. Singh, *Phys. Rev. Lett.* **79**, 733 (1997).

³⁸ K. Ishida, H. Mukada, Y. Kitaoka, K. Asayama, Z. Q. Mao, Y. Mori and Y. Maeno, *Nature* **396**, 658 (1998).

³⁹ K. Miyake and O. Narikiyo, *Phys. Rev. Lett.* **83**, 1423 (1999).

⁴⁰ Y. Sidis, M. Braden, P. Bourges, B. Hennion, S. Nishizaki, Y. Maeno and Y. Mori, *Phys. Rev. Lett.* **83**, 3320 (1999).

⁴¹ Y. Hasegawa, K. Machida and M. Ozaki, *J. Phys. Soc. Jpn.* **69**, 336 (2000).

⁴² M. J. Graf and A. V. Balatsky, *Phys. Rev. B* **62**, 9697 (2000).

⁴³ H. Won and K. Maki, *Europhys. Rev. Lett.* **52**, 427 (2000).

⁴⁴ H. Matsui, Y. Yoshida, A. Mukai, R. Settai, Y. Onuki, H. Takei, N. Kimura, H. Aoki and N. Toyota: *Phys. Rev. B* **63**, 060505 (2001).

⁴⁵ T. Nomura and K. Yamada, *J. Phys. Soc. Jpn.* **69**, 3678 (2002).

⁴⁶ T. Nomura and K. Yamada, *J. Phys. Soc. Jpn.* **69**, 404 (2002).

⁴⁷ K. Kuroki, M. Ogata, R. Arita, and H. Aoki, *Phys. Rev. B* **63**, 060506 (2002).

⁴⁸ T. Takimoto, *Phys. Rev. B* **62**, R14641 (2000).

⁴⁹ M. Sato and M. Komoto, *J. Phys. Soc. Jpn.* **69**, 3505 (2000).

⁵⁰ T. Kuwabara and M. Ogata, *Phys. Rev. Lett.* **85**, 4586 (2000).

⁵¹ Y. Hasegawa, *J. Phys. Soc. Jpn.* **67**, 3699 (1998).

⁵² M. Yamashiro, Y. Tanaka and S. Kashiwaya: *Phys. Rev. B* **56** (1996) 7847.

⁵³ M. Yamashiro, Y. Tanaka, Y. Tanuma and S. Kashiwaya, *J. Phys. Soc. Jpn.* **67**, 3224 (1998).

⁵⁴ M. Yamashiro, Y. Tanaka and S. Kashiwaya, *J. Phys. Soc. Jpn.* **67**, 3364 (1998).

⁵⁵ C. Honerkamp and M. Sigrist, *Prog. Theor. Phys.* **100**, 53 (1998).

⁵⁶ C. Honerkamp and M. Sigrist, *J. Low Temp. Phys.* **111**, 895 (1998).

⁵⁷ R. Jin, Yu. Zadorozhny, Y. Liu, D. G. Schlom, Y. Mori and Y. Maeno *Phys. Rev. B* **59**, 4433 (1999).

⁵⁸ R. Jin, Y. Liu, Z. Q. Mao and Y. Maeno, *Europhys. Lett.* **51**, 341 (2000).

⁵⁹ Y. Liu, K. D. Nelson, Z.Q. Mao, R. Jin, and Y. Maeno, Proceedings of "The International Conference on Physics and Chemistry of Molecular and Oxide Superconductors" in Taiwan (2002).

⁶⁰ A. Sumiyama, T. Endo, Y. Oda, Y. Yoshida, A. Mukai, A. Ono and Y. Onuki, *Physica C* **367**, 129 (2002).

⁶¹ P. G. de Gennes, *Superconductivity of Metals and Alloys*, (Benjamin, New York, 1966).

⁶² M. Nishida, N. Hatakenaka and S. Kurihara, *Phys. Rev. Lett.* **88**, 145302 (2002).

⁶³ L.B. Ioffe, V.B. Geshkenbein, M.V. Feigelman, A.L. Fauchere and G. Blatter, *Nature* **398**, 679 (1999).